N92-30118

THERMAL QNDE DETECTION OF AIRFRAME DISBONDS

William P. Winfree

NASA Langley Research Center

SUMMARY

Thermographic characterization of aircraft bonded lap joints offers a quick noncontacting technique to acquire information for structural integrity assessment. This paper discusses recent research to optimize the technique and determine the limits of its applicability. The temperature of the outer surface of the lap joint is increased by the application of heat flux from either flash or quartz lamp heaters. The time dependence of the surface temperature of the lap joint is imaged radiometrically. Measurements are presented for a range of specimens, ranging from samples fabricated with well characterized disbonds to actual aircraft. A technique for processing these images to enhance the contrast between bonded and disbonded regions of the lap joint is presented. Numerical models of the technique simulate the procedure. These simulations provide a cost efficient method for optimizing the technique by varying parameters such as the time for application of heat. These simulations facilitate the definition of parameters difficult to determine experimentally, such as the minimum air gap required for a disbond to be detected. Good agreement between measurements and these simulations is found.

INTRODUCTION

With the increased age of the commercial aircraft fleet, there exists a greater need for the development of new NDE techniques for the detection of critical flaws in aircraft airframes. Current techniques are considered either too time consuming or unreliable as a primary basis for integrity resulting in a requirement for major mandatory modification to the existing fleet. Improved NDE techniques offer the possibility for improved safety and reliability at reduced cost.

A major thrust of this effort is the development of large area scanning techniques. Current inspection techniques are unaided visual inspection or point measurements using a small hand held probe. Eddy current detection of cracks at rivets and sonic bond testers are characteristic of current technology being applied in maintenance facilities. These inspections are manpower intensive, requiring teams of inspectors several days to inspect the entire aircraft. Inspection reliability is reduced by human factors such as fatigue and boredom. These inspections are further compromised by the correlative basis for the techniques. Based

primarily on testing samples with fabricated defects, the ultimate reliability of the technique depends on proper fabrication of standards with defects which accurately represent in-service airframe defects.

In contrast to these techniques, much current research is focused on large area inspection techniques. A few of the areas currently under investigation are thermal imaging, acoustic emission, scanning array ultrasonics, coherent optics, radiography, magnetic field visualization and visual enhancement. Research is being pursued to develop a science base for these techniques to enable quantitative characterization of the aircraft structure. A quantitative characterization permits computer enhancement for highlighting areas of concern and reducing human factors such as fatigue and boredom. Large area scans reduce inspection time, reduce manpower cost and out of service time for the aircraft. Finally a less costly inspection improves the safety of the aircraft by economically allowing more frequent inspection.

Typical of the new large area inspection techniques is infrared thermography. Thermographic imaging does not require physical contact between the inspection system and the aircraft. The prediction of the thermal response of an aircraft has a well established science and engineering base from parallel studies to determine the thermal response of aerospace structures to given thermal loads. Infrared thermography is performed with an infrared imager capable of scanning large areas in a fraction of a second. Recent technological developments in digitized thermography have significantly increased the number of successful applications. In particular, advances in inexpensive image processors have increased the signal to noise ratio for thermographic images and enabled advances in post processing procedures. New staring array infrared imagers also have increased signal to noise relative to a single scanned detector. Thermographic imaging has an additional advantage of not requiring physical coupling between the inspection system and the aircraft.

Previous studies have shown the feasibility of thermographic techniques for detection of disbonds in bonded structures (ref. 1-7). Presented here is an overview of an effort at NASA Langley Research Center to apply thermographic techniques to the detection of disbonds in airframe lap joints. This involves computer simulation to develop a better understanding of the thermal processes particular to airframe lap joints and determine some of the limitations of the technique. Measurements are also performed on samples with both fabricated defects as well as samples removed from aircraft. Finally the technique is tested both on a NASA Langley 737 and aircraft at maintenance facilities.

COMPUTER SIMULATION OF TECHNIQUE

The thermographic technique consists of the application of heat to the surface of a structure and subsequent measurement of the surface temperatures as a function of time. To inspect a lap joint on an aircraft, the heat is applied to the exterior of the aircraft and the exterior skin temperature is measured. By heating the sample, a temperature differential is created between the lap joint regions and regions adjacent to it due to the larger heat capacity of the lap joint. For disbonded regions of the lap joint, the heat flow from the upper to lower layer of the lap joint is reduced. This reduction of heat flow is reflected in an increase in temperature over the disbonded region relative to the bonded regions.

Computer simulations of the thermographic technique were performed to help establish a better technical base for this approach. Computer simulations are a very useful tool for optimization and then determining the limitations of the technique. It is a cost effective method for considering a large variety of structures and defects. Optimization of the technique is easier since exact control can be exercised over the different parameters of interest. Examination of the sensitivity of the technique to defects which are costly and difficult to fabricate can be simulated with relative ease.

A two and three dimensional time dependent finite element heat transfer algorithm developed at Lawrence Livermore National Laboratory is used to solve the time dependence of the temperature of the structure (ref. 8). Research indicated adequate simulations require inclusion of the heat flow in the aluminum with the adhesive layer represented as a contact resistance. A disbond is simulated by increasing the contact resistance by an amount proportional to the width of the air gap forming the disbond. Details of this work are given in reference 9.

Typically the lap joint and 15.0 cm to either size of the 7.6 cm wide lap joint are included in the simulation. Since the aluminum is only 0.1 cm thick, finite element models of this structure have difficulty with large aspect ratio cells. Recent work (ref. 10) has shown this aspect ratio difficulty can be overcome by assuming a quasistatic flow condition in the aluminum, reducing the dimension of the governing partial differential equation by one. This reduced partial differential equation no longer has a large aspect ratio in the finite elements. The reduction of the dimensionality also reduces the computational time required for the simulations.

Typical results of the simulations are shown in figure 1. Initially the temperature between the bonded and disbonded regions grows as a function of time. As the temperature differential increases, a lateral heat flow develops between the bonded and disbonded regions. When the lateral heat

flow is equivalent to the applied heat flux, the temperature differential ceases to grow. This lateral heat flow reaches an equilibrium in a period of time dependent on the shape of the disbond, with smaller disbonds obtaining an equilibrium sooner than the larger disbonds. Therefore, the optimum heating protocol depends on the size and shape of the disbond. The optimum heating time for a 2.5 cm wide disbond is approximately 8 seconds.

The simulations indicate an improvement in contrast can be obtained by taking the time derivation of the thermal images. This can be seen from the time derivative for the simulation shown in figure 1. For this case the time derivative clearly shows the disbonds, in contrast to the temperature profiles the disbonds are difficult to delineate.

The advantage of simulations is clear when determining the effect of air gap width on the detectability of a disbond. For a disbond to be detectable, the air gap must be wide enough to significantly reduce the heat flow between the lap joint adherents. Fabrication of samples with varying air gaps is very difficult and expensive. However to vary the width of the air gap in the simulation is relatively easy. To determine the effect of the width of the air gap on the contrast between bonded and disbonded cases, simulations were performed keeping the size of the disbond constant. These simulations indicate a 10 μm air gap is required for significant contrast between bonded and disbonded regions.

INFRARED BOND INSPECTION SYSTEM

A schematic of the thermal measurement system is shown in figure 2. The infrared imager consists of a single liquid nitrogen cooled HgCdTe detector (8 - 12 μm). The single detector is scanned over the field of view to measure the infrared emission from the surface of the aircraft. Assuming the emissivity of the surface is 1, this signal is proportional to the temperature of the surface. If the emissivity of the surface is less than 1, the signal is a combination of the surface temperature and a reflection of background infrared images. An aluminum surface has an emissivity of less the 0.1; therefore infrared measurements of an aluminum surface yield images of the background infrared fields and not the surface temperature of the aluminum.

To overcome this difficulty, the aluminum is often coated with a thin layer of high emissivity material. Paint is typically an excellent emissivity coating, with a high emissivity regardless of the color in the 8-12 μm region. Aircraft which are painted therefore require no special treatment before inspection with the thermal inspection system. For unpainted aircraft, water washable coatings are commercially available for increasing the emissivity of the surface. The work reported here was on aircraft with either a painted surface or with a self adhering sheet applied to the aircraft. This sheet has a high

emissivity and measurements show its thermal properties as a coating were only slightly worse than those of paint.

The imager converts the infrared radiation (thermal response) from the surface of the sample to a video signal which is digitized by an image processor that performed a real time average of the digitized images. The real time averaging of these images significantly increased the signal to noise ratio of the data. Averaged images were obtained for given time series determined by the microcomputer controller. The current system allows for both immediate reduction of the data and storage of the data for further analysis.

An important feature of the system for quantitative measurements is the microcomputer which controls the data acquisition and also controls the application of heat. This enables synchronization between the heating and data acquisition. Without this synchronization it is often difficult to interpret the images obtained and impossible to obtain quantitative results. Two banks of lamps were used to heat the surface of the aircraft. Tubular quartz lamps (4000 watts) with parabolic back reflectors focused the energy onto the aircraft. These imparted ≈ 0.1 watts/cm^2 to the aircraft of interest. Flash tubes with parabolic back reflectors were used as well for heat sources. They imparted ≈ 0.2 joules/cm^2 to the aircraft in less than 1/100 of a second. For all cases considered, the temperature of the aircraft was never raised more than 10° C above ambient conditions.

MEASUREMENT RESULTS

Initial measurements were performed on laboratory standards with fabricated disbonds. The laboratory standards used, as shown in figure 3, consisted of two sheets of aluminum bonded with a three inch overlap using a room temperature cure epoxy. The dimensions of the sheets were 61 cm by 122 cm and 0.102 cm thick. Disbonds were created by inserting pull tabs (.013 cm thick) of different dimensions into the bonded region before curing. After curing, these pull tabs were then removed to leave voids in the bond.

The data obtained on these specimens was used to compare a variety of different data acquisition and reduction techniques. A cyclic heating and data acquisition protocol was determined to be most effective for detection of disbonds (ref. 11). The data was reduced by a variety of techniques such as time derivative (ref. 12) and neural networks. The neural network gave good contrast between bonded and disbonded regions; however, this requires a training of the network on either simulations of the structure or structures which are known to have disbonds. For either case, a prior knowledge of the thermal response of the structure is required. The time derivative does not require this prior knowledge, however, it is slightly less accurate in separating bonded and disbonded

regions of the lap joint.

Typical results for a laboratory standard is shown in figure 4. All of the disbonds, the smallest being 2.5 cm wide, are discernible in these images. The visual inspection of these images suggests that the contrast between the disbonded and bonded regions is greater for the 9.6 and 18.1 second heating cycles than for the 5.3 and 35.2 second cycles. Comparison of 9.6 and 18.1 second periods suggests that the contrast for the largest disbond continues to increase. However, for the 2.5 cm disbond it is questionable if the contrast is improving or degrading. A quantitative comparison shows the 9.6 second heating period is the optimum for the 2.5 cm disbond. However, for a 5 cm disbond the optimum period increases to 18.1 seconds. This variation of optimum heating time was predicted by the simulations of the technique.

Data typical of a well bonded portion of an aircraft are shown in figure 5 and 6. These images were obtained on an aircraft at a maintenance facility. In these images the bonded substructure of the airframe is clearly seen as the darker portion of the image. Outlined on these images is the substructure as determined from engineering schematics of the airframe. The bonded lap joint, tear straps and doublers above the window are all clearly seen in these images.

Images from regions with disbonded tear straps are shown in figure 7 and 8. Again outlined on these images is the extent of substructure as determined from engineering schematics of the airframe. In these images, the disbonded portions of substructure of the airframe are clearly detectable. After obtaining these images, the existence of the disbonds was verified by ultrasonic inspection and visual inspection of the interior structure.

CONCLUSIONS

Recent advances in nondestructive evaluation systems offer the possibility of increased reliability and safety at reduced cost. In particular, advances in large area scanning techniques offer significant advantages over current visual and point measurement techniques.

ACKNOWLEDGMENTS

The author would like to thank Boeing, Northwest Airlines and United Airlines for their suggestions and help in obtaining the data presented here.

REFERENCES

1. T.V. Baughn and D.B. Johnson, Materials Evaluation, vol. 44,pp 850-858, 1986.

2. P. Cielo, X. Maldague, A.A. Deom, and R. Lewak, Materials Evaluation, vol. 45,pp 452-465, 1987.

3. D.L. Balageas, A.A. Deom, and D.M. Boscher, Materials Evaluation, vol. 45, pp 461-465, 1987).

4. J. W. Maclachlan Spicer, W.D. Kerns, L.C. Aamodt and J.C. Murphy, Journal of Nondestructive Evaluation, vol. 8,pp 107-120, 1989.

5. P.K. Kuo, T. Ahmed, L.D. Favro, H.J. Hin and R.L. Thomas, Review of Progress in Quantitative Nondestructive Evaluation, edited by D.O. Thompson and D.E. Chimenti, vol. 8B, pp 1305-1310, 1989.

6. X. Maldague, J.C. Krapez, P. Cielo, and D. Poussart, Signal Processing and Pattern Recognition in Nondestructive Evaluation of Materials, edited by C.H. Chen, vol. F44,257-285, 1988.

7. W.P. Winfree and P.H. James, 35th International Instrumentation Symposium, pp 183-188, 1989.

8. A. Shapiro, "TOPAZ2D - A Two-Dimensional Finite Element Code for Heat Transfer Analysis, Electrostatics, and Magnetostatics Problems," UCID-20824. Lawrence Livermore National Laboratory, Livermore, California 94550, July, 1986.

9. P.A. Howell, W.P. Winfree, and B.S. Crews, Review of Progress in Quantitative Nondestructive Evaluation, edited by D.O. Thompson and D.E. Chimenti, vol. 10B, pp 1367-1374, 1991.

10. P.A. Howell and W.P. Winfree, Review of Progress in Quantitative Nondestructive Evaluation, edited by D.O. Thompson and D.E. Chimenti, vol. 11, 1992.

11. W.P. Winfree, B.S. Crews, and P.A. Howell, Review of Progress in Quantitative Nondestructive Evaluation, edited by D.O. Thompson and D.E. Chimenti, vol. 11, 1992.

12. W.P. Winfree B.S. Crews, H. Syed, P.H. James and K.E. Cramer, 37th International Instrumentation Symposium, pp 1097-1105, 1991.

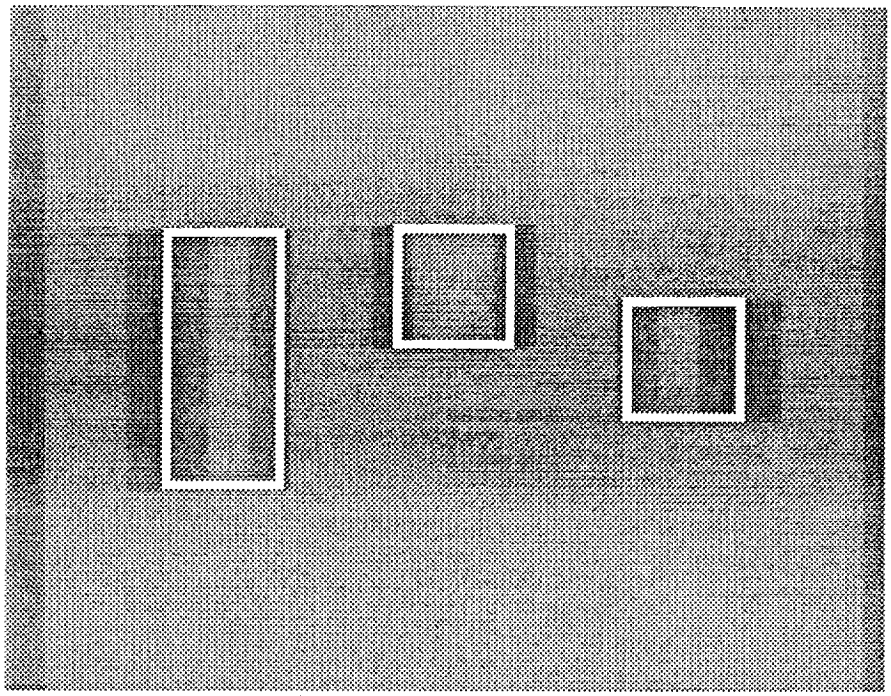

(a)

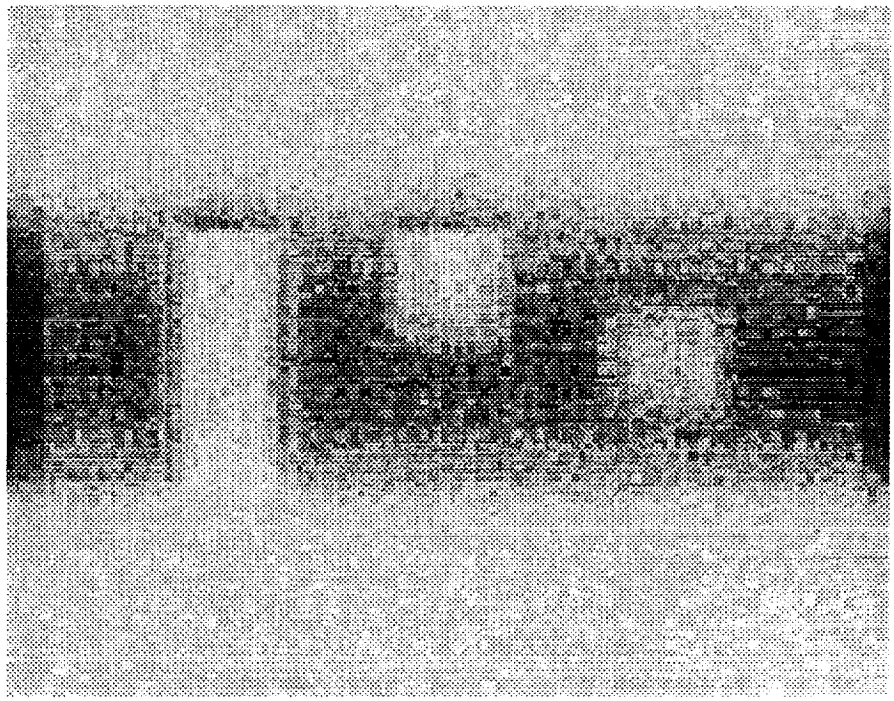

(b)

Figure 1. Typical results for simulation of thermal bond inspection system. a. The surface temperature profile for front surface heating and detection. The bond sizes are 2.5 by 7.6 cm and 2.5 by 2.5 cm and highlighted to show positions. b. The time derivative of the surface temperature clearly shows the disbonds.

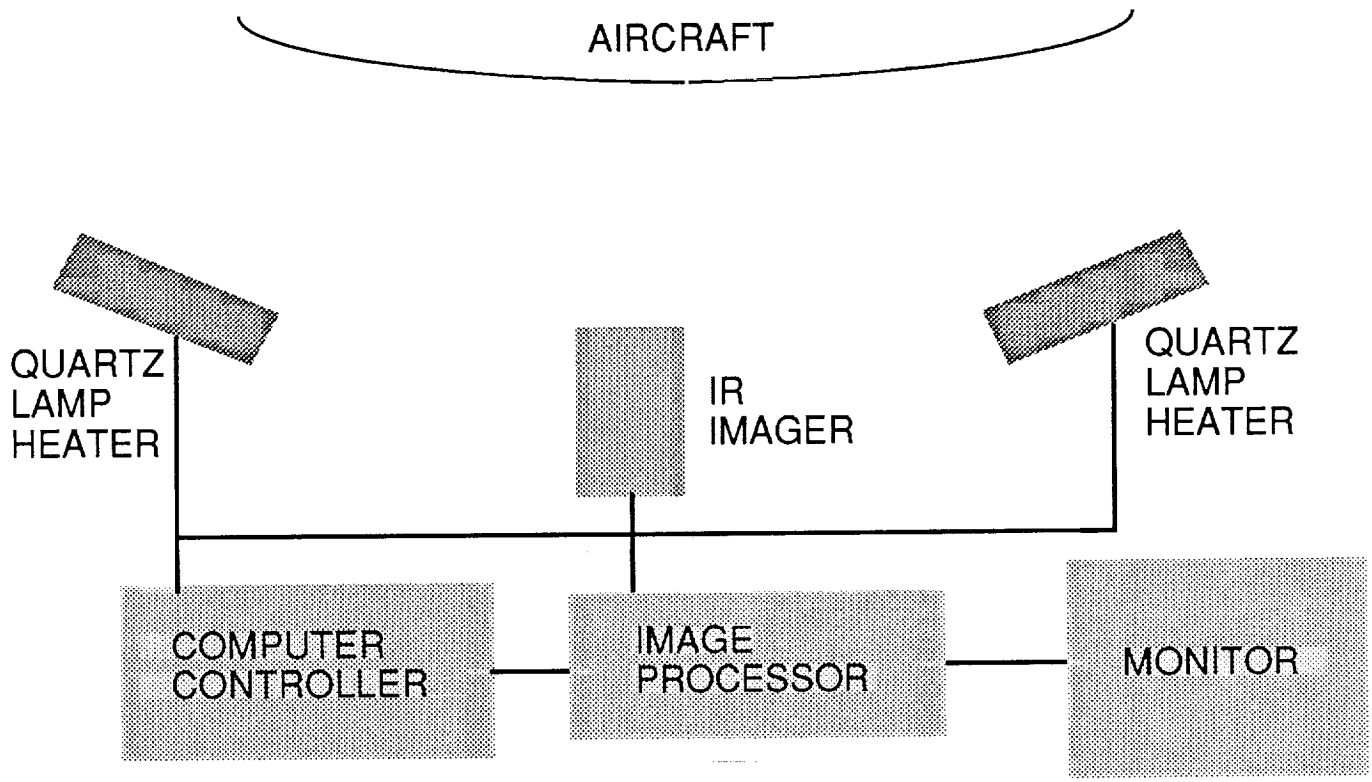

Figure 2. Schematic of thermal bond inspection system develop for field testing of thermographic technique.

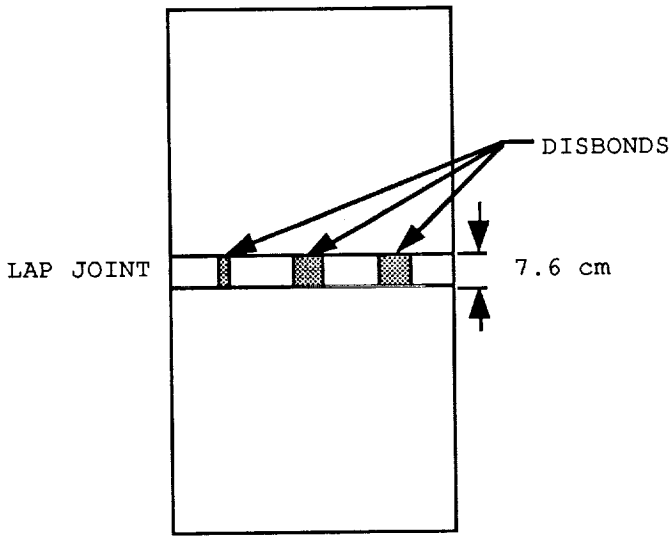

Figure 3. Typical laboratory standard configuration with two aluminum plates bonded with room cure epoxy. Disbonds are created by inserting pull tabs into over lap before bonding. These pull tabs were removed after the epoxy had cured.

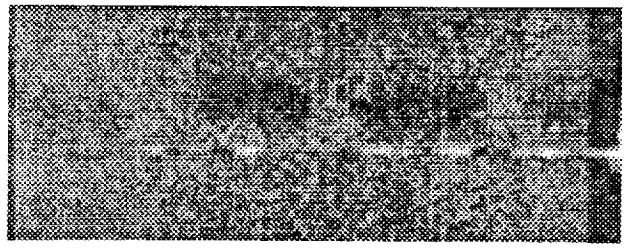

(a)

(b)

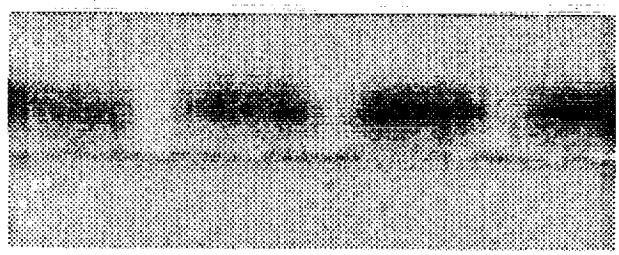

(c)

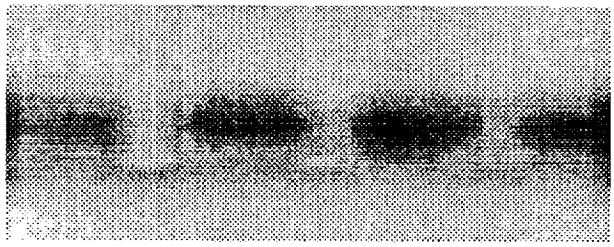

(d)

Figure 4. Typical time derivative images for a laboratory standard with 2.5, 3.8 and 5.1 cm disbonds. Heating was cyclically applied with periods of (a) 5.3, (b) 9.6, (c)18.1 and (d) 35.2 seconds.

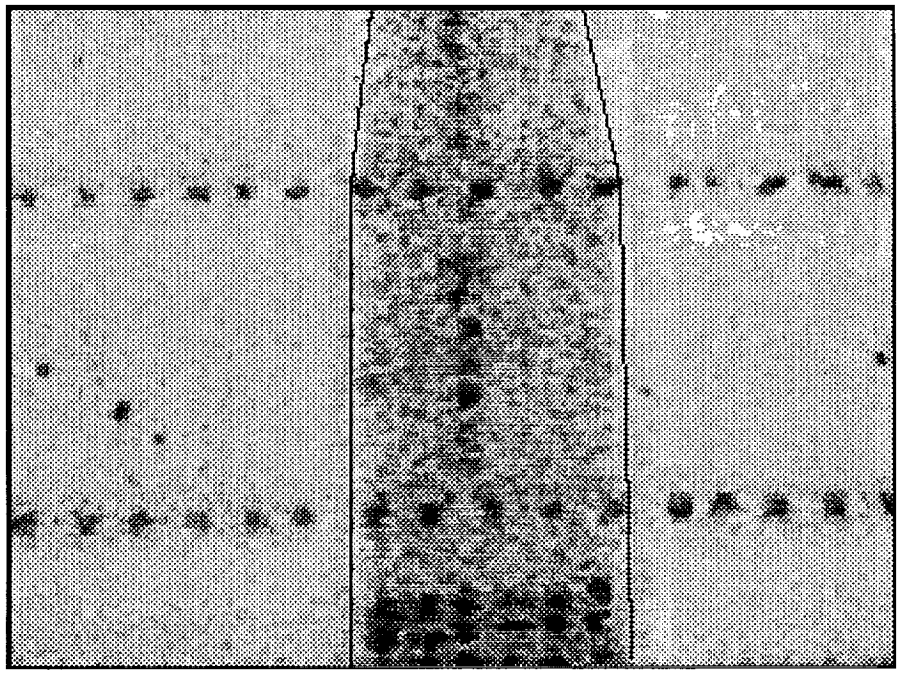

Figure 5. Images of region of airframe with no disbonds. The dark areas show regions of bonding to substructure. The substructure as determined from an engineering schematic of the airframe is outlined on the image.

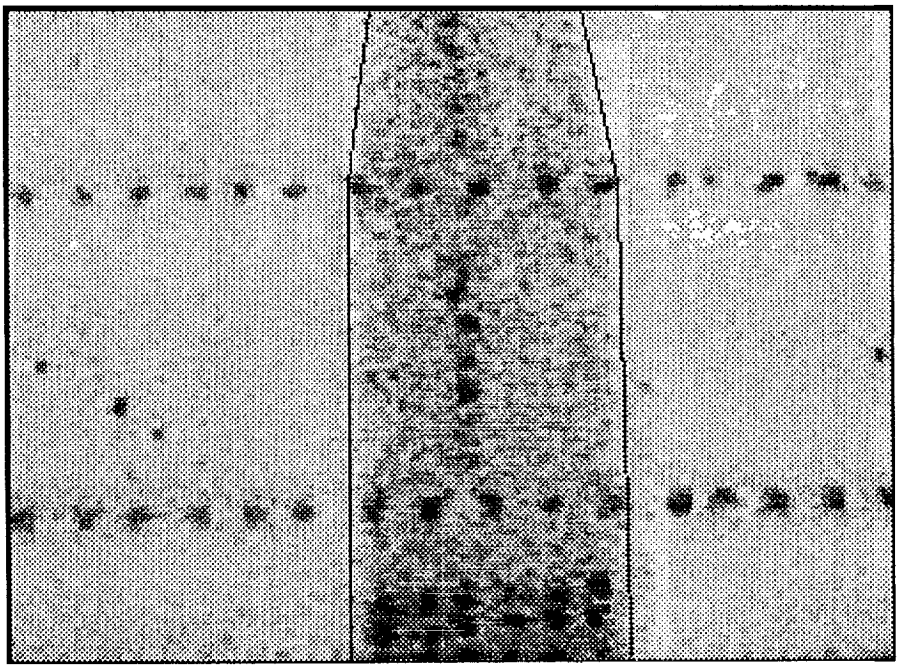

Figure 6. Images of region of airframe with no disbonds. The dark areas show regions of bonding to substructure. The substructure as determined from an engineering schematic of the airframe is outlined on the image.

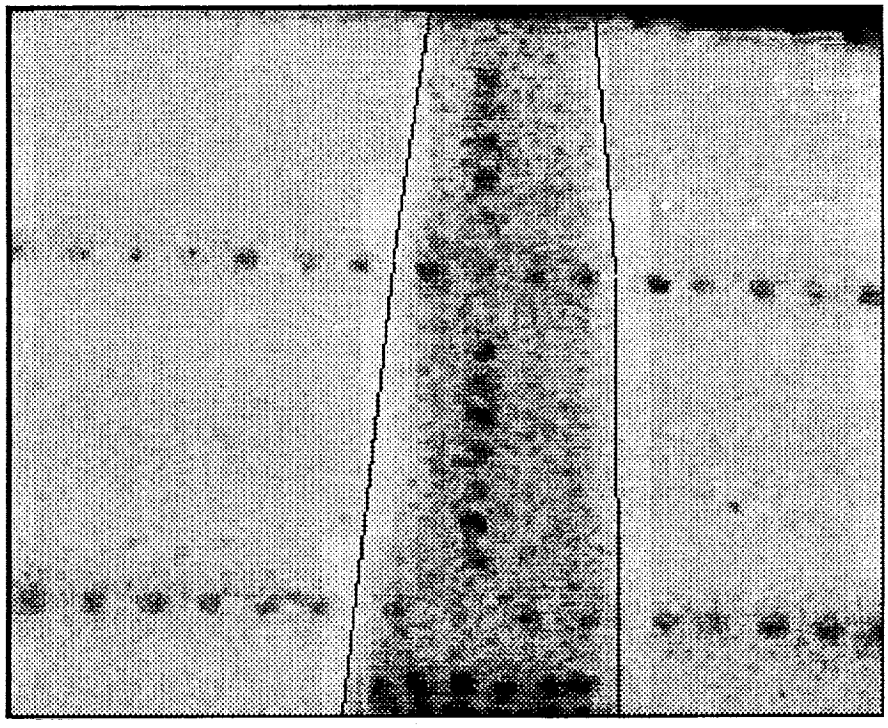

Figure 7. Images of region of airframe with disbonds. The dark areas show regions of bonding to substructure. The substructure as determined from an engineering schematic of the airframe is outlined on the image.

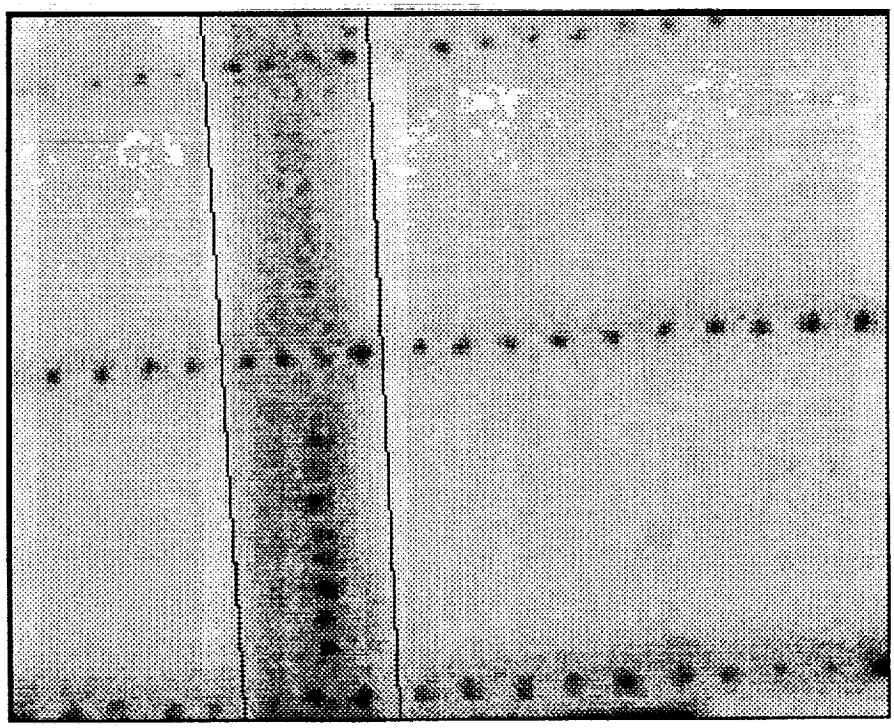

Figure 8. Images of region of airframe with disbonds. The dark areas show regions of bonding to substructure. The substructure as determined from an engineering schematic of the airframe is outlined on the image.